Radiol Phys Technol (2014) 7:277–283
DOI 10.1007/s12194-014-0261-6

Development and evaluation of statistical shape modeling for principal inner organs on torso CT images

Xiangrong Zhou · Rui Xu · Takeshi Hara · Yasushi Hirano · Ryujiro Yokoyama · Masayuki Kanematsu · Hiroaki Hoshi · Shoji Kido · Hiroshi Fujita

Received: 29 August 2013 / Revised: 6 February 2014 / Accepted: 7 February 2014 / Published online: 1 March 2014

Abstract The shapes of the inner organs are important information for medical image analysis. Statistical shape modeling provides a way of quantifying and measuring shape variations of the inner organs in different patients. In this study, we developed a universal scheme that can be used for building the statistical shape models for different inner organs efficiently. This scheme combines the traditional point distribution modeling with a group-wise optimization method based on a measure called minimum description length to provide a practical means for 3D organ shape modeling. In experiments, the proposed scheme was applied to the building of five statistical shape models for hearts, livers, spleens, and right and left kidneys by use of 50 cases of 3D torso CT images. The performance of these models was evaluated by three measures: model compactness, model generalization, and model specificity. The experimental results showed that the constructed shape models have good "compactness" and satisfied the "generalization" performance for different organ shape representations; however, the "specificity" of these models should be improved in the future.

Keywords CT images · 3D organ shapes · Statistical shape model · Point distribution model · Minimum description length

X. Zhou (✉) · T. Hara · R. Yokoyama · H. Fujita
Department of Intelligent Image Information, Division of Regeneration and Advanced Medical Sciences, Graduate School of Medicine, Gifu University, 1-1 Yanagido, Gifu 501-1194, Japan
e-mail: zxr@fjt.info.gifu-u.ac.jp

R. Xu · Y. Hirano · S. Kido
Graduate School of Medicine, Yamaguchi University, 2-16-1 Tokiwadai, Ube, Yamaguchi 755-8611, Japan

M. Kanematsu
Department of Radiology, Gifu University Hospital, 1-1 Yanagido, Gifu 501-1194, Japan

H. Hoshi
Department of Radiology, Division of Tumor Control, Graduate School of Medicine, Gifu University, 1-1 Yanagido, Gifu 501-1194, Japan

1 Introduction

The shape information on anatomic structures plays a significant role in medical image analysis. Statistical shape modeling can provide an effective way of handling the shape information by quantitatively describing the mean and possible variations of the different shapes in an observed dataset. This function of the shape model makes it possible to compare the organ shapes on different medical images objectively, and it has been applied directly to image diagnosis for detecting subtle shape changes of anatomic structures. For example, shape models were used for distinguishing the subtle differences in corpus-callosum shapes between schizophrenia patients and normal subjects [1], detecting and visualizing colonic polyps in CT colonography [2, 3], and analyzing mammographic masses [4]. In another application, shape modeling has been used widely to support region segmentations on medical images. In this purpose, the shape model is used as a shape prior or constraint for the target organ contours, and it guides the segmentation process to output such a desired final result. Much research work has been done on organ segmentation by use of shape models; a review of this work can be found in [5]. All of this previous work shows the usefulness of shape models for medical image analysis.

Several methods for statistic shape modeling such as point distribution models (PDMs) [6], m-rep and SPHARMs

[16, 17] had been reported. The PDM is a major method that has been used widely during medical image segmentations [5–7]. The basic idea of the PDM is to describe an organ shape by a number of ordered landmarks (LMs) and make a statistical analysis (finding the mean and variation of a group of LMs) based on a set of shape instances. Although the PDM proved to be useful and efficient for segmentation methods [5], the construction of a PDM still retained some difficulties, for example, how to decide correspondence of the LMs on different shape instances [6]. In fact, most related work treated these difficulties empirically and used in-house methods to construct a shape model for a special organ or purpose (a review of this work can be found in [5]). On the other hand, constructing statistic shape models needs a long time for data preparation and much technical knowledge. Therefore, a universal scheme is desired for statistical shape modeling of organ shapes, and statistical shape models for different organs that can be used directly are expected by the developments of medical image analysis. As far as we know, no shape model for an inner organ had been made available for public use, and performance evaluations of shape models for different kinds of organs on CT images still need to be done.

The motivation for this research was to develop a system which can generally construct statistical shape models for different target organs based on CT images and distribute the constructed models for other researchers. In our previous works [8, 9], we discussed and compared different methods for statistical modeling and confirmed that PDM was the most suitable approach for our purpose that focused on organ segmentation and lesion detection [8]. We also implemented an initial software package and investigated its correctness [9]. In this paper, we integrate our previous work and propose a universal scheme, which we apply to building statistical shape models for different organs by using torso CT images. Our scheme uses the points (landmarks) as the basic format to present each individual shape surface and uses a group-wise optimization method called minimum description length (MDL) to decide on the landmark correspondence between different shape instances. We describe the details of the proposed scheme and place emphasis on the model performance evaluations for different kinds of organ regions that are required by the applications. The paper is organized as follows: First, we give an overview of the scheme for the shape model construction and describe the details of the main processing steps in Sect. 2. In Sect. 3, we give the criteria for the model performance evaluations. This scheme was applied to the shape model constructions for five kinds of inner organs, and the experimental details are given in Sect. 4. The results with the discussion about the performance of the constructed shape models are given in Sect. 5. Finally, a conclusion is presented in Sect. 6.

2 Methods

In this section, we first introduce the PDM which is the basic solution for statistical shape modeling and then give an overview of the proposed system for constructing a 3D PDM for organ regions based on CT images.

2.1 Point distribution modeling for 3D organ regions

A statistical shape model is designed for presenting the mean geometry of a specific organ shape and some statistical modes of the shape variation from a training set of the shape instances. The PDM is a general shape modeling approach that relies on the landmark points on the target organ contour to present the organ shapes [6]. Given a training set (n annotated organ regions), we can get $\mathbf{x}_1,\ldots,\mathbf{x}_n$ vectors from each set. Each $\mathbf{x} = (x_1, y_1, z_1, \ldots, x_l, y_l, z_l)$ has l aligned landmarks with the image coordinates x, y, z and sufficiently approximates the geometry of the shape of the corresponding organ region. Under the condition that landmarks with the same index in different shape instances $\mathbf{x}$ represent the same anatomic location, the mean shape and shape variation can be calculated by the following steps:

(1) Compute the mean shape $\bar{\mathbf{x}}$.

$$\bar{\mathbf{x}} = \frac{1}{n}\sum_{i=1}^{n}\mathbf{x}_i \tag{1}$$

(2) Compute the shape variation $\mathbf{M}$:

$$\mathbf{M} = \frac{1}{n-1}\sum_{i=1}^{n}(\mathbf{x}_i - \bar{\mathbf{x}})(\mathbf{x}_i - \bar{\mathbf{x}})^{\mathrm{T}} \tag{2}$$

(3) Using singular value decomposition (SVD) to decompose the $\mathbf{M}$ as

$$\mathbf{M} = \mathbf{U}\sum\mathbf{U}^{\mathrm{T}} \tag{3}$$

where $\mathbf{U}$ is a matrix whose column vectors represent the set of orthogonal modes (eigenvectors $\boldsymbol{\varphi}_i$) of shape variation $\mathbf{M}$, and $\boldsymbol{\Sigma}$ is a diagonal matrix of corresponding singular values ($\sqrt{\lambda_i}$, where $\lambda_i$are the eigenvalues)

(4) An estimate of a novel shape, $\mathbf{y}$, of the same organ can be represented by the mean shape $\bar{\mathbf{x}}$ and a line combination of k ($1 \le k \le n$) principal modes $\boldsymbol{\varphi}_i$ with the coefficients α_i as

$$\mathbf{y} \cong \bar{\mathbf{x}} + \sum_{i=1}^{k}\alpha_i\varphi_i. \tag{4}$$

In this way, a shape instance $\mathbf{y}$ can be quantitatively represented or analyzed based on a set of coefficients α_i, where α_i is the parameter of PDMs and can be calculated by the inner product of the $\mathbf{y}$ and $\boldsymbol{\varphi}_i$. We can generate a new shape $\mathbf{y}$ by adjusting the parameter α_i which is governed by

the underlying probability distribution of the training shapes. Such a probability distribution can usually be assumed to be a Gaussian distribution; thus, α_i is set to the values within the range of $[-3\sqrt{\lambda_i}, 3\sqrt{\lambda_i}]$ in order to make sure that the new generated shape is acceptable.

2.2 System overview

In this research, we developed a system that can be used generally for construction of statistical shape models for presenting the different organ surfaces based on the PDM approach. An overview of the proposed system is shown in Fig. 1. The input of the system is a training set of 3D CT images, and the output is a statistical shape model for a specific organ region.

Our system provides a graphic user interface to help operators to segment the target organ region in each CT image. We developed a semi-automatic method for this interface by using 2D manual seed-point inputting with a 3D organ extraction approach [10]. After the organ shapes are obtained from the CT images, the system automatically constructs a statistical shape model to present the shapes of the extracted organs. The processing flow of the system includes four steps, as shown in Fig. 1. Through these steps, the organ regions on CT images are transferred from voxel-based regions to mesh-based surfaces first, and then, vertices of the meshes are used for construction of the PDM that presents the organ shapes in all of the inputted CT images. The details of the processing procedure in each step are described in the following sections.

2.2.1 *Semi-automatic organ region segmentation*

The target organ region in each CT image was segmented by use of a graphic interface that was developed by our research group [10]. Instead of manually inputting the contour of the target organ region, our system only requires the operator to indicate the coordinates of some pixels (seed points) inside and outside the organ region on the 2D images, and the computer automatically segments the 3D target organ region by using the positions of these seed points. The details of the algorithms for organ segmentations used in this interface can be found in [10].

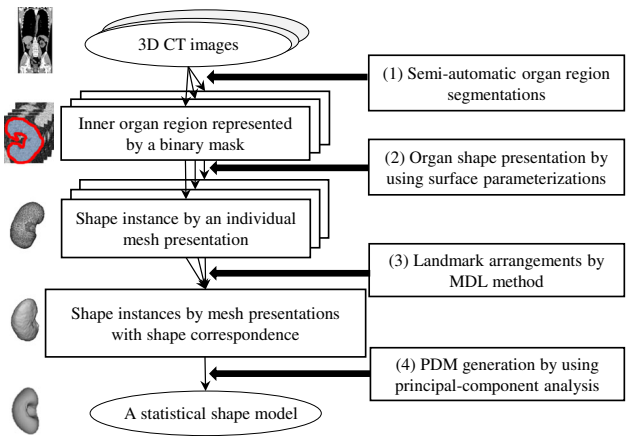

Fig. 1 Processing flow of shape modeling

2.2.2 *Organ shape presentation by use of surface parameterizations*

The organ region is represented by a group of voxels in CT images after the segmentation process. The shape is defined by the contour of the organ region that appears as a closed three-dimensional surface. Instead of using of all of the voxels of the contour, only a number of landmarks that approximate the global shape smoothly are selected and used for shape modeling. In this system, we generate a number of triangle meshes from the contour voxels by first using a matching cubes algorithm [11], we then smooth the mesh surface and merge the adjacent meshes iteratively to reduce the vortex number of the meshes to a pre-defined constant k by using the Visualization ToolKit [12]. Finally, the organ shape that originally appears as all of the contour voxels on CT images is represented by a comparatively lesser number of vertices of the surface meshes.

2.2.3 *Landmark arrangements by use of the MDL method*

Given n shape instances of training samples, each shape is represented by vertices of meshes obtained in the previous step. In order to construct the statistical shape models, we need to seek a set of landmarks (coordinates of l points) $\mathbf{x}_i$ $(i = 1, 2, \ldots, l)$, located at the corresponding parts on these n shapes. The determination of the corresponding landmarks can be generalized as a problem of shape alignment, which eliminates spatial differences of shapes caused by pose parameters (translation, orientation, and scaling) in different CT cases.

In this system, an MDL-based method [13] has been used for accomplishing the landmark arrangements. Because the landmarks of a group of shapes are determined simultaneously, the MDL method is also called a group-wise based method. The intent of the MDL method is to find a set of landmarks which lead to statistical shape models describing the training samples as efficiently as possible. The efficiency of the model is defined by an objective function of the MDL, D, that is calculated based on the eigenvalues λ_i in Eq. (3). The best landmark correspondence over all of the training samples can be obtained by minimizing of D to lead a compact model for describing all of the shapes in the training samples [13].

In practice, we project all meshes to a unit spherical surface based on the conformal mapping method to remove the differences in translation and scaling among shape instances first, and then rotating those meshes on the spherical surface to eliminate orientation differences by minimizing the MDL's function D [13]. A gradient-descent optimization method [14] is used for seeking the location of the minimum value of the function D quickly.

2.2.4 PDM generation by use of principal component analysis

When the landmarks $\mathbf{x}_i$ of the n training shapes are determined, a PDM that presents the average and possible variations of the organ shapes can be generated by use of the traditional approach described in Eqs. (1)–(3), based on principal component analysis.

3 Performance evaluation for statistical shape models

The performance of a shape model was measured by three criteria: compactness, generalization, and specificity, that reflect the performance in being easy to handle, and having shape expression capability and correctness for shape predictions for a statistical shape model [13].

Compactness shows the model efficiency that aims to use a smaller number of model parameters to handle larger variations of the shape instances. The compactness C is defined as

$$C = \sum_{i=1}^{k} \lambda_i. \tag{5}$$

Here, k is the number of principal modes $\boldsymbol{\varphi}_i$ used in statistical shape models, and λ_i is an eigenvalue from Eq. (3). Intuitively, a compact model is more useful for practical applications that desire to handle all of the shape instances by a few parameters.

Generalization is the model ability for presenting the novel shape instances of the target organ that are not used during model construction. The generalization ability G is defined as the cumulative difference between the novel shape instance and its shape representation based the shape model. If we have n shape instances for testing the model generalization by using a leave-one-out method and each shape instance is presented by a landmark set $\mathbf{x}$, then G can be written as

$$G = \frac{1}{N-1} \sum_{i=1}^{n-1} \|\mathbf{x}_i - \mathbf{y}_i\|. \tag{6}$$

Here, $\mathbf{y}_i$ is the shape representation of $\mathbf{x}_i$ that calculated by Eq. (4) based on a shape model constructed by the other $n-1$ shape instances. Intuitively, a model that has a smaller G can present a new shape instance more accurately.

Specificity measures the validation of the shape instances that are presented by the model. The specificity can be calculated by randomly generating a number of shapes from the model and measuring the differences between each generated shape instance with its nearest neighbor (a shape instance that has the shortest Euclidean distance to a referred shape) in the model space that is used for model construction. If we generate a number of instances $\mathbf{x}_i$ ($i = 1,\ldots,C$) on a model space and each instance $\mathbf{x}_i$ can find a nearest neighbor $\mathbf{x}'_i$ that is really used for model construction, the specificity S can be defined as

$$S = \frac{1}{C} \sum_{i=1}^{C} \left\|\mathbf{x}_i - \mathbf{x}'_i\right\|. \tag{7}$$

Intuitively, a smaller S means that an arbitrary prediction based on a shape model will generate a shape that looks like one of the shape instances in the training set.

An ideal shape model should be compact, have the ability to present all of the validated shape instances correctly (smaller G), and should not deliver any invalidated shape instances (smaller S). Measuring such performances for a constructed shape model is important and required by the developments of the applications on CT images.

4 Experiment

This system was applied to the shape model construction for different inner organs by use of 3D CT images. Five kinds of organ regions, including hearts, livers, spleens, and right and left kidneys, were used as the targets. We randomly selected 50 patient cases (CT images) with normal organ shapes as the training set. Each CT image covered the whole human torso by $512 \times 512 \times 798$–$1{,}104$ voxels with an image resolution of 0.625 (mm) in three directions. A 16-detector CT scanner (Lightspeed 16; GE Healthcare, Milwaukee, WI, USA) with a fixed tube voltage of 120 kVp and an automatic tube current modulation program (3D mA Modulation; GE Healthcare) was used for generating each CT scan. The CT parameters were set as follows: collimation, 1.25 mm; detector configuration, 16 detectors with 1.25 mm section thickness (16×1.25 mm); noise index, 9.8; table feed, 27.5 mm per rotation; pitch, 1.37; 75 cm craniocaudal scan range; 32 cm field of view; 0.5 s gantry rotation time; and 14.2 s scan acquisition time. Breath-hold CT scans were obtained and CT images were reconstructed at 1.25-mm-thickness sections, by use of a standard reconstruction algorithm. Five organ regions in each CT image were extracted manually based on mutual consent of the first and second

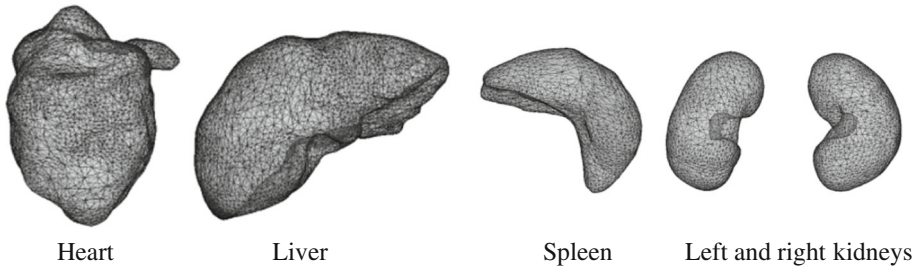

Fig. 2 Extraction results for five organ surfaces in a CT case

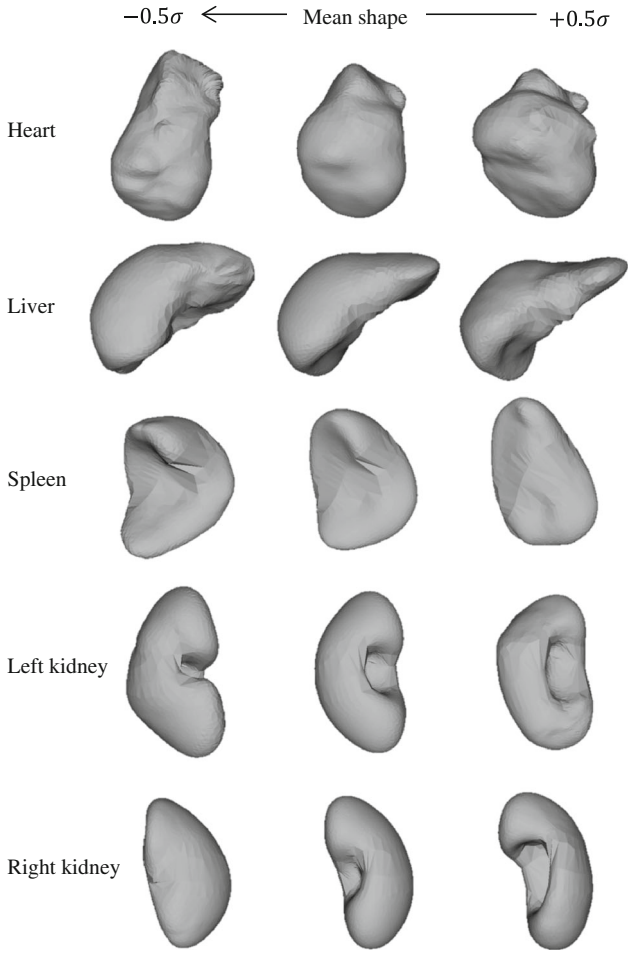

Fig. 3 Shape instances delivered from the statistical shape models for five kinds of organs (shapes on *left* and *right* sides are generated by Eq. 4 by using parameters $k = 1$; $a_1 = \pm 0.5\sigma$; $\sigma = \sqrt{\lambda_1}$)

authors under the instructions of a medical expert (author 5). Figure 2 shows an example of the 3D views of the organ surfaces of five target organs in one case.

The shape model constructions were carried out for each organ independently. The number of shape instances n for model training was 50. The number of landmarks l for the final PDMs was fixed at 2,562 empirically, based on the expressiveness of these LMs for different organ shapes. The mean shapes and their variations for each target organ are shown in Fig. 3. The constructed models were evaluated by measurement of the performance of the compactness, generalization, and specificity. The evaluation results are indicated in Fig. 4.

5 Results and discussions

We confirmed that the proposed system can construct statistical shape models for presenting the typical shapes of principal organs. The mean shape for each organ was reasonable under the anatomic definition, as shown in the middle column of Fig. 3. By changes in the values on each mode, the constructed shape model can deliver a sequence of shape instances.An example of the shape variances by changing the value of the first mode were shown on the left and right sides of Fig. 3. The heart shapes showed a larger variance, and the shape variance of the liver was relatively smaller. Those shape variances should be affected by the patient individual differences and curvature distributions of different organ surfaces. These results showed that the proposed system can be used for constructions of statistical shape models for the principal inner organs based on 3D CT images.

As shown in Fig. 4, we found that the values of compactness, generalization, and specificity of the shape models varied largely within 1–10 modes, and there was almost no change beyond 20 modes. Actually, most applications based on shape models cannot handle more than 10 modes for parameter optimization; the compactness of the constructed models is suitable for practical applications.

For the evaluation results of the generalization (Fig. 4c), we confirmed that the minimum values of G of the models were distributed around 20–40 mm (a cumulative error of 2,562 landmarks) for different organs. Considering that the spatial resolution of the CT images was 0.625 mm, a displacement with an average around 0.01–0.02 voxel occurred in each landmark between the surfaces delivered from the original CT images and the representation of the models. This accuracy should be high enough for supporting the automatic organ segmentation that was the main application of the organ shape modeling.

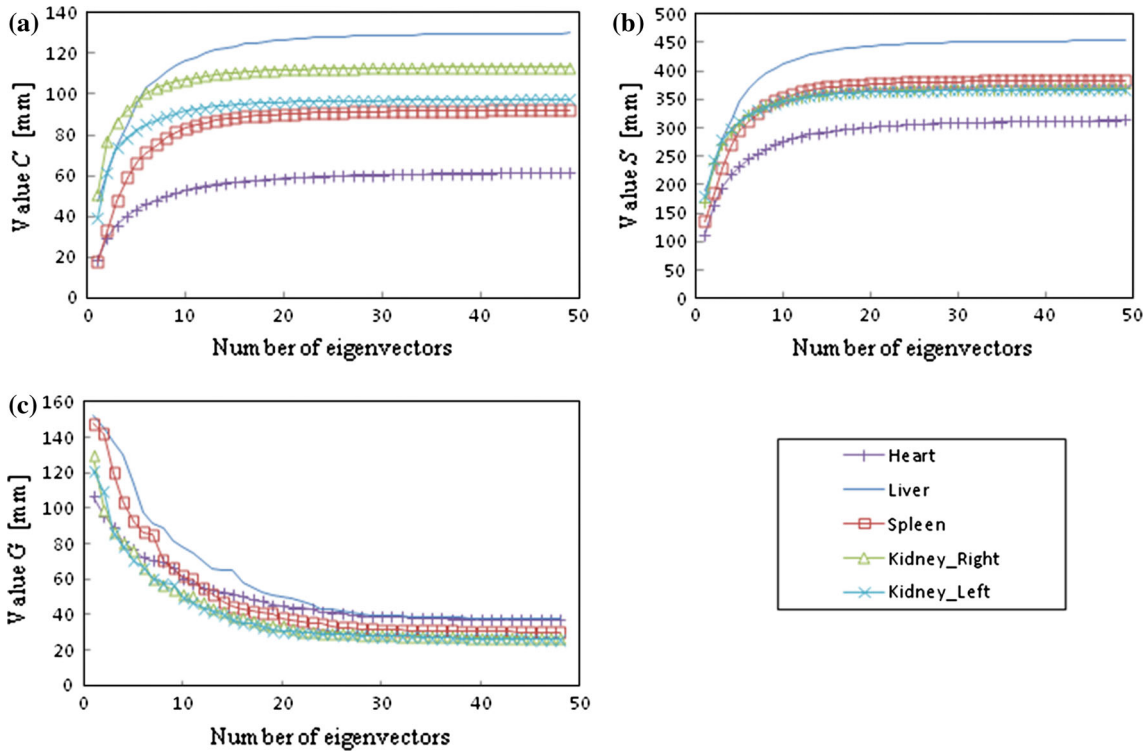

Fig. 4 Performance evaluations of constructed five shape models in terms of **a** compactness C, **b** specificity S, and **c** generalization G

For the specificity, we found that the performance of the models was not good enough. As shown in Fig. 4b, the errors (S defined in Eq. 7) were distributed from 300 to 450 mm. This result showed that the shapes delivered randomly from the models had a large difference to the instances in the training set. Some of those shapes generated by the models were also judged as inadequate upon inspection by the authors.

The performance of the specificity was affected by landmark correspondence, which is the most important part of shape modeling. The MDL method was used for solving the correspondence, based on the implicit inference that the compact model is the best one. This consideration led to a compact model, but there is no evidence to prove theoretically and explicitly that a compact model will also provide a good correspondence of the landmarks in anatomy, which may cause a worse performance regarding specificity. This problem showed that accuracy of the shape representation from the anatomy aspect should be considered as a new measure for evaluating the model performance in medical purposes. Although a paper recently reported an improved MDL method [15], it is still an open question how to fill the gaps between the theory of a compact model in MDL and anatomic correspondence of landmarks in practice. In addition, how to balance all of the measures (compactness, generalization, and specificity) during the statistical shape modeling for different inner organs is another question that remains for the future work.

6 Conclusion

In this research work, we proposed a system for constructing statistical shape models based on CT images. This system was applied to 50 cases of torso CT images for constructing five shape models for the heart, liver, spleen, and right and left kidneys. The experimental results showed that the proposed system can construct a compact model to represent these organ shapes efficiently and correctly compared to the original shapes on CT images. However, the validity of the shapes that were delivered from the models randomly was not good enough, and improvement of the model specificity should be considered in future work.

Acknowledgments The authors thank members of the Fujita Laboratory. This research work was funded in part by a Grant-in-Aid for Scientific Research on Innovative Areas, and in part by a Grant-in-Aid for Scientific Research, MEXT, Japan.

Conflict of interest The authors declare that they have no conflict of interest.

References

1. Frumin M, Golland P, Kikinis R, Hirayasu Y, Salisbury DF, Hennen J, Dickey CC, Anderson M, Jolesz FA, Grimson WE, McCarley RW, Shenton ME. Shape differences in the corpus callosum in first-episode schizophrenia and first-episode psychotic affective disorder. Am J Psychiatry. 2002;159:866–8.
2. Nappi J, Frimmel H, Yoshida H. Virtual endoscopic visualization of the colon by shape-scale signatures. Inf Technol Biomed IEEE Trans. 2005;9:120–31.
3. Yoshida H, Nappi J, MacEneaney P, Rubin DT, Dachman AH. Computer-aided diagnosis scheme for detection of polyps at CT colonography. Radiographics. 2002;22:963–79.
4. Berks M, Caulkin S, Rahim R, Boggis C, Astley S. Statistical appearance models of mammographic masses. Proc IWDM. 2008;2008:401–8.
5. Heimann T, Meinzer H. Statistical shape models for 3D medical image segmentation: a review. Med Image Anal. 2009;13:543–63.
6. Cootes T, Taylor C, Cooper D, Graham J. Active shape models—their training and application. Comput Vision Image Underst. 1995;61:38–59.
7. Cootes T, Hill A, Taylor C, Haslam J. The use of active shape models for locating structures in medical images. Image Vis Comput. 1994;12:355–66.
8. Yamaguchi S, Zhou X, Xu R, Hara T, Yokoyama R, Kanematsu M, Hoshi H, Kido S, Fujita H. Construction of statistical shape models of organs in torso CT scans using MDL method. Proc Int Forum Med Imaging Asia. 2012;2012:2–33.
9. Xu R, Zhou X, Hirano Y, Tachibana R, Hara T, Kido S, Fujita H. Evaluation of group-wise based methods for statistical shape models construction. Japanese Society of Medical Imaging Technology 2011. 2011; CD-ROM, OP1-7.
10. Yamagichi S, Hayashi T, Zhou X, Hara T, Yokoyama R, Kanematsu M, Hoshi H, Fujita H. An interactive method for organ region segmentation in X-ray CT images, Japanese Society of Medical Imaging Technology 2011. 2011; CD-ROM, OP1-8.
11. William EL, Harvey EC. Marching Cubes: a high resolution 3D surface construction algorithm. Comput Graph. 1987;21:163–9.
12. The Visualization Toolkit (VTK). http://www.vtk.org. Accessed 25 Feb 2014.
13. Davies R, Twining C, Cootes T. A minimum description length approach to statistical shape modeling. IEEE Trans Med Imaging. 2002;21:525–37.
14. Heimann T, Wolf I, Williams T, Meinzer H. 3D active shape models using gradient descent optimization of description length. Proc IPMI'05. 2005; 3565:566–77.
15. Xu R, Zhou X, Hirano Y, Tachibana R, Hara T, Kido S, Fujita H. Particle-system based adaptive sampling on spherical parameter space to improve the MDL method for construction of statistical shape models. Comput Math Methods Med. 2013;2013:1–9, Article ID 196259.
16. Pizer SM, Fletcher PT, et al. Deformable m-reps for 3D medical image segmentation. Int J Comput Vision. 2003;55:85–106.
17. Székely G, Kelemen A, Brechbühler C, Gerig G. Segmentation of 2-D and 3-D objects form MRI volume data using constrained elastic deformations of flexible Fourier contour and surface models. Med Image Anal. 1996;1:19–34.